Cite as: Russo B.; Franciosa P. eat al. "Towards real-time physics-based variation simulation of assembly systems with compliant sheet-metal parts based on reduced-order models", International Joint Conference on Mechanics, Design Engineering and Advanced Manufacturing, Ischia (Naples – Italy), 2022

Towards real-time physics-based variation simulation of assembly systems with compliant sheet-metal parts based on reduced-order models

Abstract. Variation Simulation (VS) allows early validation and certification of the assembly process before parts are built. State-of-the-art VS models of assembly systems with compliant sheet-metal parts are based on Finite Element Method (FEM) integrated with statistical approaches (i.e., Monte Carlo simulation). A critical technical barrier is the intense computational cost. This paper proposes a novel real-time physics-based VS model of assembly systems with compliant sheet-metal parts based on Reduced-Order Model (ROM). Compared to the literature on the topic, this study reports the first application of a ROM, developed for VS by using both intrusive and non-intrusive techniques.

The capability of the proposed method is illustrated in a case study concerning the assembly process of the vertical stabiliser for commercial aircrafts. Results have shown that the accuracy of ROM (based on proper orthogonal decomposition) depends on the sampling strategy as well as on the number of reduced modes. Whilst a large CPU time reduction by several orders of magnitude is achievable by non-intrusive techniques (based on radial basis functions for interpolation), intrusive models provide more accurate results compared to the full-order models.

Keywords: real-time physics-based simulation, variation simulation analysis, sheet metals, compliant assembly, reduced-order models, proper orthogonal decomposition, radial basis functions.

Nomenclature

VS	Variation Simulation	K_{FOM}	Stiffness matrix of the FOM
FOM	Full Order Model	F_{FOM}	Load vector of the FOM
ROM	Reduced Order Model	k_p	Penalty stiffness
μ	Vector of input parameters	ε_{gap}	Gap tolerance
u	Output performance indicators	N_P	Number of parameters
T_μ	Constraints on input parameters	N_S	Number of sampled points
T_u	Constraints on output indicators	N_{DOF}	Number of Degrees of Freedom
u_s^i	Displacement of the i-th slave node	S_{snap}	Snapshot matrix
u_{s-m}^i	Displacement of the projection of the i-th slave node on master surface	Ψ	Reduced basis
		R	Number of retained modes
P_s^i	i-th slave node	u_{ROM}	Displacement vector of the ROM
P_{s-m}^i	Projection of i-th slave node on the master surface	K_{ROM}	Stiffness matrix of the ROM
		F_{ROM}	Load vector of the ROM
N_c	Normal vector of the master element	POD	Proper Orthogonal Decomposition
g_{init}	Initial gap between P_s^i and P_{s-m}^i	RBF	Radial Basis Function
u_{FOM}	Displacement vector of the FOM	MPE	Mean Percentage Error

1 Introduction

Combining high strength with the ability to be formed and cut with good dimensional accuracy at relatively low cost, sheet-metal parts are widely employed in automotive and aerospace applications as exterior panels and interior structural components. However, the intrinsic flexibility of these parts adds variability to the process, since real (non-ideal) compliant parts need to be clamped and forced to the targeted assembly position before fastening operations. Consequently, assembled panels tends to spring back once fastening tools are released [1].

Variation Simulation (VS) techniques allow simulating the generation and propagation of variations throughout the assembly process, thus enabling early validation and certification even before assemblies are built. State-of-the-art VS models of assembly systems with compliant sheet-metal parts are based on Finite Element Method (FEM) integrated with statistical approaches (i.e., Monte Carlo simulation or polynomial chaos [2]). VS methods have been used to accelerate strategies for *right-first-time* and digitalisation of the manufacturing process [3]. The mechanistic models for VS can be grouped into two main categories: (1) *VS-based analysis* and (2) *VS-based synthesis*.

VS-based analysis addresses the problem of finding the effect of input parameters on output performance indicators, under specific design constraints; whereas, the reverse problem is faced by the VS-based synthesis. Most of the publications have been addressing problems related to VS-based analysis but fewer attempts have been made to develop efficient models to face the VS-based synthesis. Urged by the need to reduce defects and waste during manufacturing, VS-based synthesis has become a critical priority since allows product and process optimisation at early design stages.

VS-based synthesis covers topics related to process optimisation, parametric and sensitivity analyses [1–7]. The common denominator is the desire to generate accurate results in a reasonable time (ideally in real-time), which is sometimes not achievable due to the complexity of the problem even with powerful computational systems (High Performance Computing - HPC, cloud computing, etc.). In fact, typical VS applications involve a large number of input parameters (up to 1,000 for a typical body-in-white assembly process in automotive) related to both product and process. The leading challenge is driven by the dimensionality of the design space. For instance, finding global optima in high-dimensional problems is extremely challenging since the number of evaluations required to explore the design space increases exponentially with its dimensionality (this is also known as the “curse of dimensionality”). Several authors have been facing this problem. For example, the optimisation algorithm developed by Xing [4], who optimised the location of locators for an inner hood assembly, took 1,687 hours to ensure the global best solution. Aderiani et al. [5] applied a new method to optimise the fixture layout to two simple single-station cases, elapsing 110 hours and 160 hours, respectively. Sinha et al. [6] proposed a Deep Learning-based methodology to aid multiple root causes analysis for an assembly process. To train their Deep Neural Network (DNN), they conducted 9 runs of 10,000 FEM simulations by varying the positions of only 5 clamps.

Other approaches implement the Response Surface Methodology (RMS), which, trained on a pre-existing dataset, aims at obtaining a model that can be deployed to solve the optimisation problem [7]. Unfortunately, RSM approaches are pure data-driven and they are regarded as "black-box" models in the sense that they can find complex non-linear patterns on tested/trained cases. However, they are unable to explain the cause-effect mechanisms between variables and outside of the training dataset.

Recently, the Reduced-Order Models (ROM) have been applied to solve computational intense problems, such as fluid-structure interaction problem [8], computational fluid-dynamics [9] and structural dynamics [10]. ROM methods are attractive since they allow reducing the dimensionality of the model. ROM techniques compute off-line the solution of several complete Full-Order Models (FOM) and extract the modes that best describe the solution to the full problem. Therefore, differently from RSM, ROM techniques exploit the known physical behaviour represented by the modes. The number of such modes determines the ratio between accuracy and computational time. Finding the right balance between accuracy and computational efficiency is an open topic and will be discussed in this paper.

This paper proposes a novel methodology to accelerate the transition towards real-time physics-based variation simulation of assembly systems with compliant sheet-metal parts. This is the first time that a ROM approach is developed for VS using both intrusive and non-intrusive techniques.

The novelty of the paper is twofold: (1) implementation of a ROM approach to enable real-time VS of compliant sheet-metal parts; (2) integration of ROM with Active Set Method for contact modelling and thus avoid part-to-part penetration. The paper extends the work of Lindau et al. [11] who proposed to combine the method of influence coefficients [12] with a simplified contact search algorithm. However, this method was only limited to triangular mesh elements and node-to-node contact modelling. The approach proposed in our paper goes beyond the state-of-the-art since is independent of the mesh density and implements a node-to-surface contact model.

The reminder of the paper is as follows: Section 2 describes the problem formulation. Section 3 shows the proposed methodology. Section 4 presents the case study along with results and discussions. Section 5 concludes the paper with future opportunities.

2 Problem formulation

2.1 Representation of the VS model

A typical VS model conceptually involves finding the relationship between input parameters, μ, and output performance indicators, u, under specific design constraints, T. Input parameters define the design space and may be related to both the product (e.g., shape errors) and the process (e.g., positioning errors, shape and position of clamps, etc.). The mechanistic model for variation propagation can be conceptually represented as in equation (1), where f embeds the physics-based model to simulate the compliancy of the sheet-metal parts and to avoid part-to-part penetration.

$$\begin{cases} u = f(\mu) \\ \text{s.t.: } \mu \subseteq T_\mu \text{ and } u \subseteq T_u \end{cases} \tag{1}$$

2.2 Physics-based model and computational challenges

The physics-based model is based on a FEM kernel and the following modelling assumptions are made: (i) points which are candidate to come in contact are computed once on the un-deformed structure, according to the *node-to-surface* search method [13], shown in Fig. 1(a); and, (ii) frictionless contact between mating surfaces. For each i-th iteration, the displacements of all potential points belonging to the slave part are constrained to those of the master part as in equation (2) (see also Fig. 1(b)), where u_s^i and u_{s-m}^i are the displacements of the slave vertex P_s^i and its projection on the master part, P_{s-m}^i, respectively; N_c is the normal vector of the master element, and g_{init} is the initial gap of the contact pair.

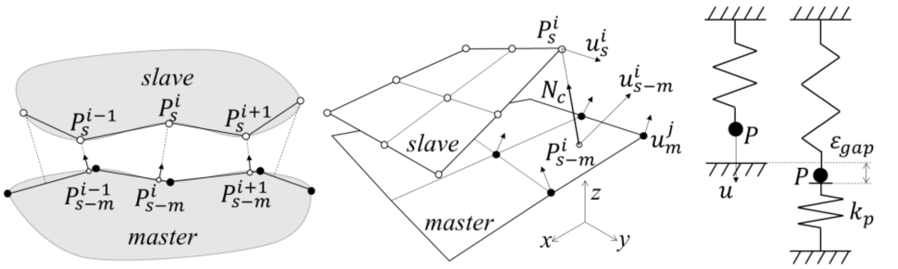

Fig. 1. Representation of the part-to-part contact model.

The constitutive non-linear equations are defined in equation (3), where u_{FOM} is the primary variable (both master and slave), F_{FOM} is the load vector, and K_{FOM} is the stiffness matrix.

$$\begin{cases} g_{init} = (P_s^i - P_{s-m}^i) \cdot N_c \\ g_{init} + N_c \cdot (u_s^i - u_{s-m}^i) \geq 0 \end{cases} \quad (2)$$

$$K_{FOM}(u_{FOM}, \mu) \cdot u_{FOM}(\mu) = F_{FOM}(u_{FOM}, \mu) \quad (3)$$

Equations (2-3) constitute the Full-Order Model (FOM). In this paper, the Penalty method has been implemented to enforce the conditions in (2). Other methods (such as Lagrange Multipliers) are possible but for the sake of demonstrating the methodology, we have limited the formulation only to the Penalty method. The solution u_{FOM} of equation (3) is obtained by the Active Set Method: the model is iteratively solved by activating the contact pairs only where there has been part-to-part penetration (i.e., negative gaps) in the previous iteration. This translates to the fact that the active pairs are moved away by enabling the penalty stiffness, k_p (see Fig. 1(c)). The solution converges only if the gaps of all the active contact pairs are lower than a pre-set gap tolerance, ε_{gap}, and all pairs are in compression (negative load). Since the Penalty method tends to approximate the conditions in equation (2), the accuracy of the solution is highly influenced by the choice of the penalty stiffness itself. The case study will show the sensitivity to the selection of the penalty stiffness.

Since VS-based synthesis involves a large set of input parameters and also the need to recompute the stiffness matrix itself (due, for example, to variations in material properties), the solution of equations (2-3) would require a prohibitive amount of time. This paper aims at providing accurate solutions of the VS model in equations (2-3) and with a significant reduction in computational time.

3 Proposed methodology

The methodology is hinged on a ROM approach and combines both intrusive [14,15] and non-intrusive [8,10] methods. Intrusive methods act directly on the constitutive equations defined in (3) and they aim at reducing the time spent to perform each iteration of the non-linear set of equations. Conversely, non-intrusive techniques build a surrogate model in a hybrid space and the solution to any un-tested configuration of the input parameters is obtained by interpolating the surrogate model. As such, non-intrusive techniques do not require modifications of the constitutive equations as opposed to intrusive techniques.

Since those two approaches have pros and cons, this paper has implemented both to explore their full potential. Details of the methodology (Fig. 2) are:

OFF-line stage (training): this stage is intended for generating the training dataset. **Step (1) Define *parameter space*, $\boldsymbol{\mu}$.** The parameter space, whose dimensionality is N_P, is sampled (N_S is the number of sampled points) using various techniques, such as uniform, random, full factorial or Latin hypercube. **Step (2) Generate *snapshots*, $\boldsymbol{u_{FOM}}$ (full-order model).** For each sample in the parameter space, a specific solution of *u* is obtained from the FOM model in equations (2-3). Each solution is named *snapshot*. The full set of solutions are then stored in the *Snapshot matrix*, $S_{Snap} = \left[u_{FOM}(\mu_1), \dots, u_{FOM}\left(\mu_{N_S}\right)\right] \in \mathbb{R}^{N_{DOF} \times N_S}$, where N_{DOF} is the number of degrees of freedom of the FOM. The snapshot matrix is represented in the field space. **Step (3) Generate *field space* & compute *reduced basis*, $\boldsymbol{\Psi}$.** This is the core step of the methodology and a reduced basis $\Psi \in \mathbb{R}^{N_{DOF} \times R}$ is computed by extracting from the snapshot matrix R orthogonal modes that represent the most significant patterns hidden in the field space.
ON-line stage (deployment): Ψ is used to reduce the dimensionality of the model for each new parameter instance, $\mu^{(d)}$, not sampled during the OFF-line stage. **Step (4) Intrusive method** **Step (4.1) *Forward projection* of constitutive equations.** The constitutive equations in equation (3) are projected into the reduced space, lowering the dimensionality from N_{DOF} to $R \ll N_{DOF}$, thus obtaining the reduced stiffness matrix $K_{ROM} \in \mathbb{R}^{R \times R}$ and reduced load vector $F_{ROM} \in \mathbb{R}^{R \times 1}$. **Step (4.2) Solve *reduced* model, $\boldsymbol{u_{ROM}^{(d)}}$.** The result of the projection is the system of non-linear equations (4), which for instance, defines the reduced-order model:

$$K_{ROM}(u_{FOM}, \mu) \cdot u_{ROM}(\mu) = F_{ROM}(u_{FOM}, \mu) \tag{4}$$

where $u_{ROM} \in \mathbb{R}^{R\times 1}$ is the reduced solution. Being the dimensionality R lower than N_{DOF}, the inversion of K_{ROM} is much faster than FOM in equations (2-3).

Step (5) Non-intrusive method

Step (5.1) *Forward projection* of snapshots. The snapshots are projected into the reduced basis. Opposed to step (4.1), no manipulation of the constitutive equations is required.

Step (5.2) Compute *interpolation*, $\boldsymbol{u_{ROM}^{(d)}}$. A surrogate model is built within the hybrid space which maps the parameter space into the reduced space.

Step (6) *Backward projection* and *approximated* solution. This is the final step, common to both intrusive and non-intrusive methods, and the reduced solution is back-projected into the field space.

Table 1. Main features of the implemented ROM methods.

		Intrusive ROM	**Non-intrusive ROM**
OFF-line stage	Step (2)	$S_{Snap} = [u_{FOM}(\mu_1), \dots, u_{FOM}(\mu_{N_s})]$	
	Step (3)	Singular Value Decomposition (SVD) and truncation	
ON-line stage	ROM solution	**For each iteration (step 4.2):** $u_{ROM}(\mu) = inv(K_{ROM}(u_{FOM}, \mu)) \cdot F_{ROM}(u_{FOM}, \mu)$	**1-off solution (step 5.2)** interpolated $u_{ROM}(\mu)$
	Approximated solution (step 6)	**For each iteration** $u_{FOM}(\mu) \cong \Psi \cdot u_{ROM}(\mu)$	**1-off solution** $u_{FOM}(\mu) \cong \Psi \cdot u_{ROM}(\mu)$

Implementation steps and hurdles of the two methods are summarised in Table 1. It is worth noting that if, on one hand, the non-intrusive ROM generates a surrogate model of u, the intrusive ROM needs to re-run the physics-based kernel and the constitutive equations must, therefore, be projected during each iteration.

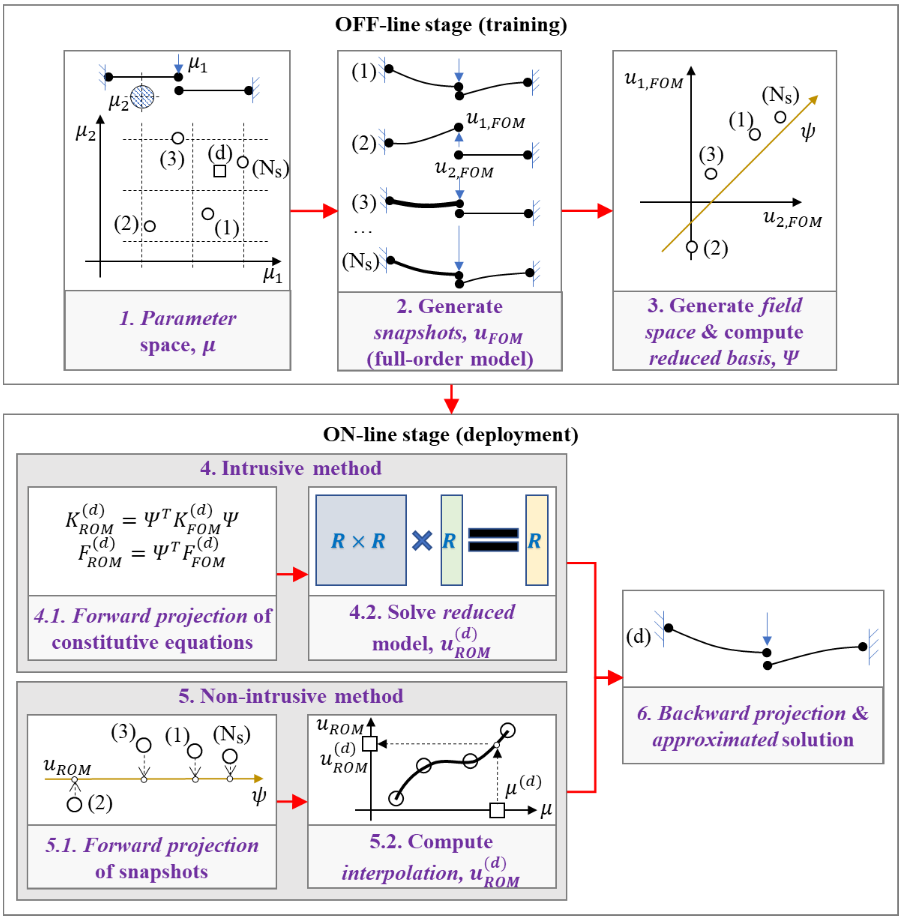

Fig. 2. Proposed methodology for real-time physics-based variation simulation.

4 Case study

4.1 Implementation

The implementation of the proposed methodology uses the Proper Orthogonal Decomposition (POD) [9,14–16], since it has proven to be advantageous in terms of easiness of implementation, reduction of computational cost, and accuracy of results. POD methods rely on the SVD (Singular Value Decomposition) of the Snapshot matrix $S_{Snap} = U\Sigma V^T$ and extract the reduced basis by collecting the first R left singular vectors $\Psi = U(:,1:R)$, namely, the POD-modes of the system. Its intrusive version [9,15] is generally called *POD-Galerkin*, taking its name from the projection. The non-intrusive version, called *POD-RBF* [9,16], uses the Radial Basis Functions (RBF) to interpolate the approximated solution in the hybrid space. The methodology has been coded in MATLAB® R2020b and the adopted physics-based simulations have been calculated in the Variation Response Method (VRM) toolkit [17,18]. All calculations have been run on a laptop with 12 GB of RAM and a quad-core CPU operating at Max Turbo Frequency of 3.60 GHz.

4.2 Description of the case study: aircraft vertical stabilizer

The methodology has been tested on the vertical stabiliser of a commercial aircraft, shown in Fig. 3. The assembly comprised of 2 skins (left- and right-handed), 1 rib, 14 clips, and 9 rib posts. All components are made from aluminium, with Young's modulus 70 GPa and Poisson's ratio 0.3. The model has been discretized with 20,497 shell elements (Fig. 3(b)), resulting in N_{DOF}=128,644.

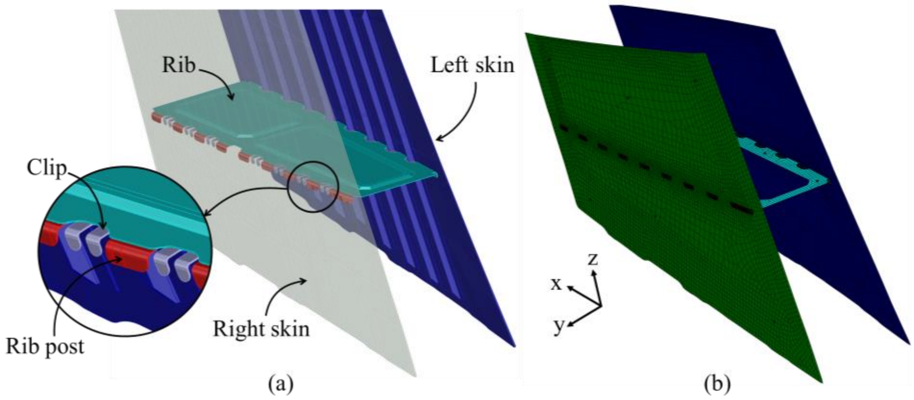

Fig. 3. Vertical stabilizer. (a) CAD geometry and (b) mesh of the selected assembly.

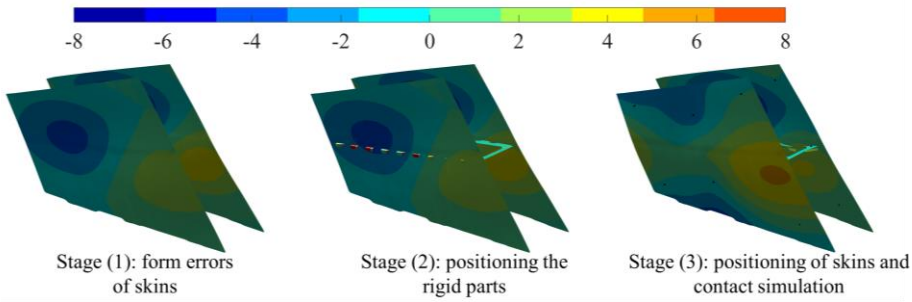

Fig. 4. Deformation field (in mm) during the 3 consecutive assembly stages. Deformation has been magnified 5 times. The colour code represents the y displacements in mm.

The assembly process is modelled with three consecutive stages (shown in Fig. 4 for a given instance of the input process parameters): *stage (1)* incoming skins are deformable and are subject to form errors – the Morphing Mesh Procedure (MMP), developed in [11] has been used to emulate form errors. It is worth noting that the methodology works regardless and scanning data can be also fed to the model. *Stage (2)* positioning of rib, clips, and rib posts which are assumed rigid. *Stage (3)* positioning of the skin panels and contact simulation. The output performance indicators are the deformation field (in x, y, and z axis) for each node in the mesh model.

Table 2. Definition of the input parameters.

Input parameters, μ		Uniform Distribution	Gaussian Distribution	
		Interval	Mean	Std. deviation
Form errors	Normal deviation of 3 control points of the left skin	$[-5mm, 5mm]$	$0mm$	$1.67mm$
	Normal deviation of 3 control points of the right skin	$[-5mm, 5mm]$	$0mm$	$1.67mm$
Z-rotation of Rib Post 1÷9		$[-5mm, 5mm]$	$0mm$	1.67°

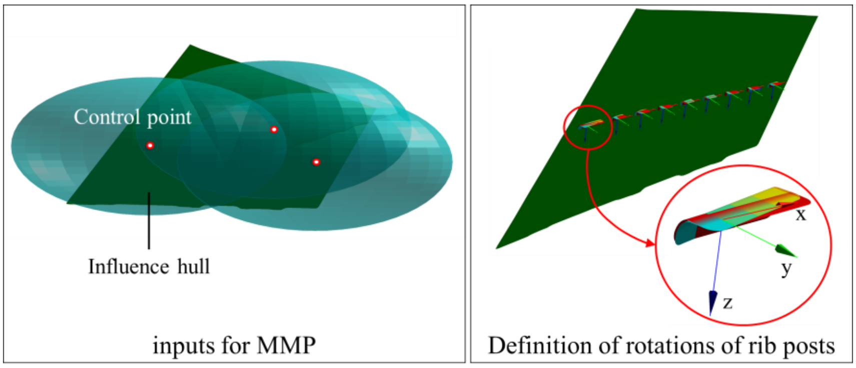

The parameter space comprises 15 parameters (Table 2). Two sampling strategies have been used, unform and gaussian, both with N_S=640. The snapshots were generated by setting ε_{gap}=0.6 mm. Results of the model reduction are then tested against 60 new instances of process parameters, generated with uniform random sampling. The accuracy is quantified by 3 indicators: (1) Mean Percentage Error (MPE) and the (2) Pearson's Correlation coefficient over all the 60 new instances computed between FOM and ROM solutions. The (3) CPU time ratio (i.e., time spent by the ROM compared to the FOM) measures the computational efficiency.

4.3 Results

Preliminary tests showed that the accuracy of the intrusive method is strongly influenced by the penalty stiffness (Fig. 5). It was found that when the penalty is relatively low (approx. 10^2 N/mm), the solution converges without respecting the gap tolerance, while it fails to converge for penalty stiffness above 10^7 N/mm. Only for k_p=[10^4; 10^6] N/mm there is good accuracy (MPE below 0.3%) with significant reduction in computational time – up to 50% saving. The results presented hereinafter have been generated by setting the penalty stiffness, k_p=10^5 N/mm.

Fig. 6 shows the results of the sensitivity study on the number of modes against the sampling strategy. While the general trend is that the MPE tends to exponentially decrease with the increasing number of modes, better accuracy is reached with the uniform sampling. This is explained by the fact that, compared to the gaussian sampling, the uniform sampling allows to scan the entire parameter space. The next set of results has been generated using uniform sampling.

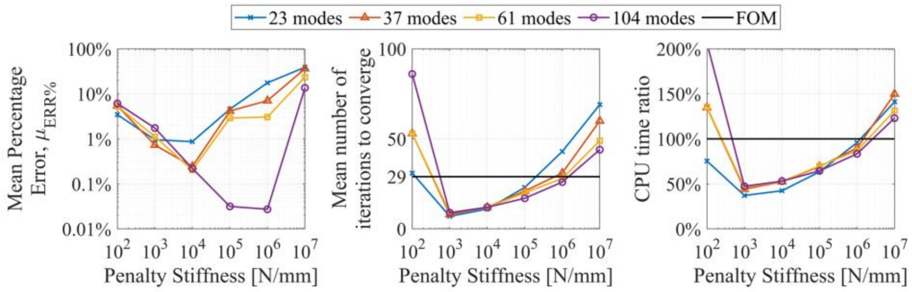

Fig. 5. Sensitivity to penalty stiffness for the POD-Galerkin method.

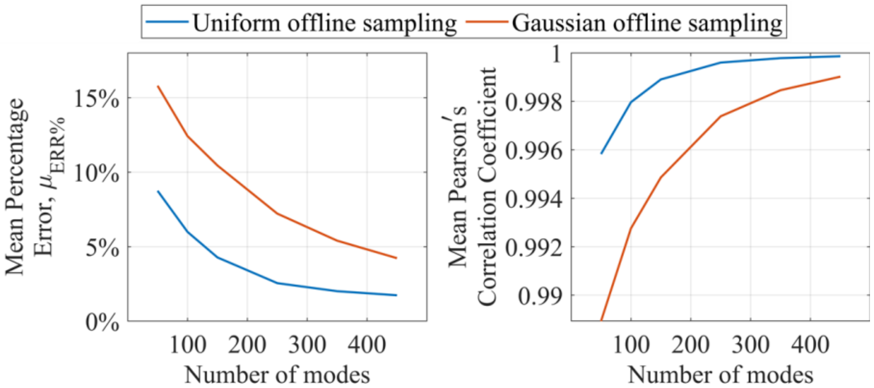

Fig. 6. Sensitivity to no. of modes with both uniform and gaussian sampling for POD-Galerkin.

Fig. 7 depicts the contour plots of the displacements and errors along y-axis of the right skin for 2 different parameter instances, while Fig. 8(a) shows the results in terms of errors and pattern reproducibility via Pearson's Correlation coefficient. Results of the POD-Galerkin with less than 50 modes are not shown since the reduced model exhibited convergence problems. Conversely, POD-RBF error reaches a plateau just after 10 modes, indicating that the reduced basis does not have enough information to represent the entire variability in the field space. Further reduction in error could be achieved by increasing the number of sampled points in the parameter space. It is therefore clear that the intrusive method, with the same number of modes and sampled points, is more accurate than the non-intrusive counterpart.

With regards to the computational efficiency, Fig. 8(b) shows the CPU time ratio for the major steps of POD-Galerkin. It is clear that the *forward projection* is the bottleneck of the procedure, and the CPU time ratio increases with the increasing number of modes. Summary of findings is in Table 3.

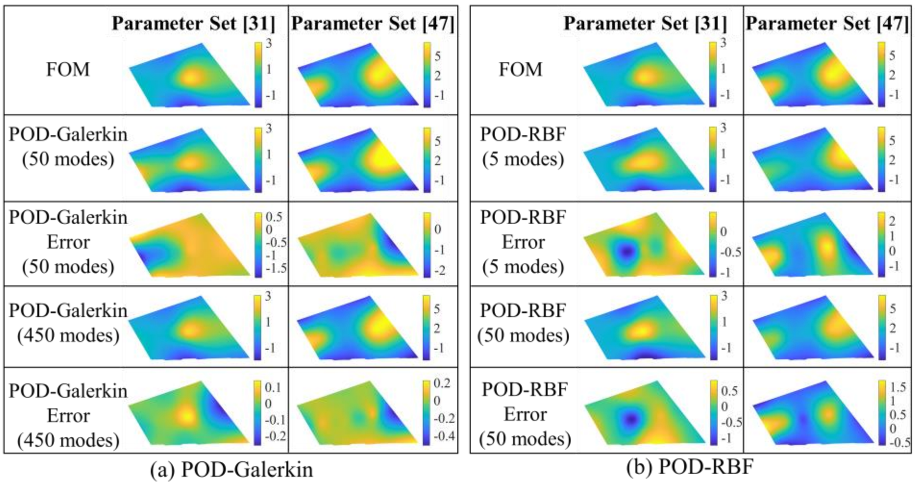

Fig. 7. Comparison between the FOM, POD-Galerkin and POD-RBF. The colour code represents the displacements (mm) and errors (mm) along y-axis of the right skin for two instances of parameters.

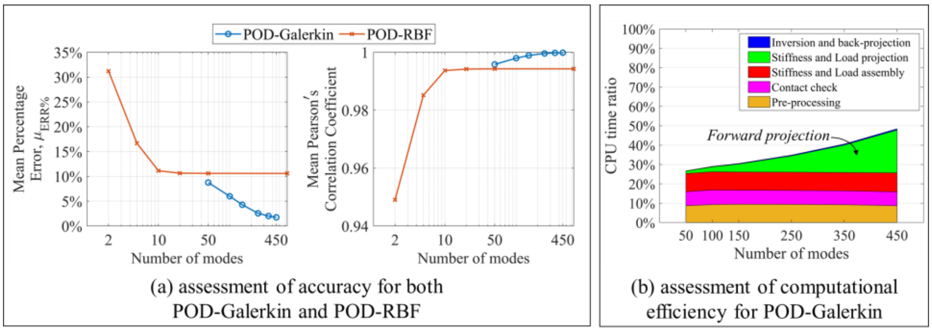

Fig. 8. Comparison between the POD-Galerkin and POD-RBF in terms of accuracy and computational efficiency.

Table 3. Summary of the main findings in terms of accuracy and computational efficiency.

Models		Computational time	CPU time ratio	Mean Percentage Error
FOM		3,000 s	-	-
POD-Galerkin	50 modes	830 s	27.7%	8.7%
	450 modes	1,500 s	50%	1.7%
POD-RBF	5 modes	2.5 s	0.09%	16.7%
	50 modes	2.5 s	0.09%	10.6%

5 Conclusions

This paper proposed a novel methodology to accelerate the transition towards real-time physics-based variation simulation of assembly systems with compliant sheet-metal parts. Results have shown that the accuracy of the proposed Reduced-Order Model for variation simulation strictly depends on the number of input parameters and sampled points, as well as the sampling strategy and the number of reduced modes. Further, though intrusive methods are much more accurate than the non-intrusive counterpart since they exploit the physical knowledge in the reduced space, they are limited only up to 4x reduction (with MPE just below 10%) of computational time compared to Full Order Models. Conversely, non-intrusive methods can go as high as 1000x. However, their accuracy is dictated by the number of sampled points.

This paper represents the first attempt to bridge the gap between advanced CAE simulations and VS models with the final aim of generating simulation data in real-time. This research has opened interesting new avenues in the field of variation simulation and dimensional/quality management. Opportunities for hybrid approaches based on ROM and physics-driven Machine Learning will be explored in future works.

References

1. A. Das, P. Franciosa, D. Williams, and D. Ceglarek, "Physics-driven Shape Variation Modelling at Early Design Stage," in *Procedia CIRP*, 2016, vol. 41.
2. P. Franciosa, S. Gerbino, and D. Ceglarek, "Fixture Capability Optimisation for Early-stage Design of Assembly System with Compliant Parts Using Nested Polynomial Chaos Expansion," in *Procedia CIRP*, 2016, vol. 41.
3. P. Franciosa and D. Ceglarek, "Hierarchical synthesis of multi-level design parameters in assembly system," *CIRP Annals - Manufacturing Technology*, vol. 64, no. 1, 2015.
4. Y. F. Xing, "Fixture Layout Design of Sheet Metal Parts Based on Global Optimization Algorithms," *J Manuf Sci Eng*, vol. 139, no. 10, 2017.
5. A. Rezaei Aderiani, K. Wärmefjord, R. Söderberg, L. Lindkvist, and B. Lindau, "Optimal design of fixture layouts for compliant sheet metal assemblies," *Int J Adv Manuf Tech*, vol. 110, no. 7–8, 2020.
6. S. Sinha, E. Glorieux, P. Franciosa, and D. Ceglarek, "3D convolutional neural networks to estimate assembly process parameters using 3D point-clouds," in *Multimodal Sensing: Technologies and Applications*, 2019, vol. 11059, pp. 89 – 101.
7. S. Gerbino, P. Franciosa, and S. Patalano, "Parametric variational analysis of compliant sheet metal assemblies with shell elements," in *Procedia CIRP*, 2015, vol. 33.
8. D. Xiao, P. Yang, F. Fang, J. Xiang, C. C. Pain, and I. M. Navon, "Non-intrusive reduced order modelling of fluid-structure interactions," *Comput Methods Appl Mech Eng*, vol. 303, 2016.
9. S. Georgaka, G. Stabile, K. Star, G. Rozza, and M. J. Bluck, "A hybrid reduced order method for modelling turbulent heat transfer problems," *Computers and Fluids*, vol. 208, 2020.
10. M. Karamooz Mahdiabadi, P. Tiso, A. Brandt, and D. J. Rixen, "A non-intrusive model-order reduction of geometrically nonlinear structural dynamics using modal derivatives," *Mech Syst Signal Process*, vol. 147, 2021.

11. B. Lindau, S. Lorin, L. Lindkvist, and R. Soderberg, "Efficient contact modeling in nonrigid variation simulation," *J Comput Inf Sci Eng*, vol. 16, no. 1, 2016.
12. S. Charles Liu and S. Jack Hu, "Variation simulation for deformable sheet metal assemblies using finite element methods," *J Manuf Sci Eng*, vol. 119, no. 3, 1997.
13. P. Wriggers, "Computational Contact Mechanics," 2nd edn. Wiley, 2003.
14. F. Chinesta, A. Huerta, G. Rozza, and K. Willcox, "Model Reduction Methods," in *Encyclopedia of Computational Mechanics Second Edition*, 2017.
15. M. R. Pfaller, M. Cruz Varona, J. Lang, C. Bertoglio, and W. A. Wall, "Using parametric model order reduction for inverse analysis of large nonlinear cardiac simulations," *Int J Numer Meth Biomed Engng*, vol. 36, no. 4, 2020.
16. V. Buljak, *Inverse Analyses with Model Reduction Proper Orthogonal Decomposition in Structural Mechanics*, vol. 33. 2012.
17. P. Franciosa and D. Ceglarek, "VRM simulation toolkit. Available on line: http://www2.warwick.ac.uk/fac/sci/wmg/research/manufacturing/downloads/," 2016.
18. P. Franciosa, A. Palit, S. Gerbino, and D. Ceglarek, "A novel hybrid shell element formulation (QUAD+ and TRIA+): A benchmarking and comparative study," *Finite Elem Anal Des*, vol. 166, 2019.